Microtubule Stabilization in Pressure Overload Cardiac Hypertrophy

Hiroshi Sato, Toshio Nagai, Dhandapani Kuppuswamy, Takahiro Narishige, Masaaki Koide, Donald R. Menick, and George Cooper IV

Cardiology Section of the Department of Medicine and the Department of Physiology, Gazes Cardiac Research Institute, Medical University of South Carolina and the Veterans Administration Medical Center, Charleston, South Carolina 29401

Abstract. Increased microtubule density, for which microtubule stabilization is one potential mechanism, causes contractile dysfunction in cardiac hypertrophy. After microtubule assembly, α-tubulin undergoes two, likely sequential, time-dependent posttranslational changes: reversible carboxy-terminal detyrosination (Tyr-tubulin ↔ Glu-tubulin) and then irreversible deglutamination (Glu-tubulin → Δ2-tubulin), such that Glu- and Δ2-tubulin are markers for long-lived, stable microtubules. Therefore, we generated antibodies for Tyr-, Glu-, and Δ2-tubulin and used them for staining of right and left ventricular cardiocytes from control cats and cats with right ventricular hypertrophy. Tyr-tubulin microtubule staining was equal in right and left ventricular cardiocytes of control cats, but Glu-tubulin and Δ2-tubulin staining were insignificant, i.e., the microtubules were labile. However, Glu- and Δ2-tubulin were conspicuous in microtubules of right ventricular cardiocytes from pressure overloaded cats, i.e., the microtubules were stable. This finding was confirmed in terms of increased microtubule drug and cold stability in the hypertrophied cells. In further studies, we found an increase in a microtubule binding protein, microtubule-associated protein 4, on both mRNA and protein levels in pressure-hypertrophied myocardium. Thus, microtubule stabilization, likely facilitated by binding of a microtubule-associated protein, may be a mechanism for the increased microtubule density characteristic of pressure overload cardiac hypertrophy.

We have shown on the levels of sarcomere and cardiac muscle cell, or cardiocyte, that a persistent increase in microtubule density accounts to a remarkable degree for the contractile dysfunction seen in pressure overload hypertrophy of the right ventricle (RV)[1] (Tsutsui et al., 1993, 1994). This discovery had its genesis both in theoretical considerations (Hill and Kirschner, 1982) and in experimental observations (Joshi et al., 1985) suggesting that an extending force, such as that exerted on the cardiocyte by cardiac pressure loading, could rapidly shift the dynamic equilibrium between free and polymerized tubulin toward the polymerized form. However, our previous work showed that while load modulation of the set point of the tubulin–microtubule equilibrium may be partially responsible for the induction and persistence of increased microtubule density, other factors acting in a less direct manner during and after hypertrophic growth are also likely to be operative (Tagawa et al., 1996). In particular, the fact that microtubule density increases only after hypertrophic growth is initiated (Tagawa et al., 1996) suggested microtubule stabilization as an attractive candidate explanation for this phenomenon.

To explore this hypothesis, we took advantage of the fact that the α-tubulin moiety of the αβ-tubulin heterodimer, once assembled into a microtubule, undergoes two posttranslational modifications, such that the prevalence in microtubules of the first and then the second of these modified forms of α-tubulin serves as a clock indicating microtubule age. The first modification is a reversible carboxy-terminal detyrosination by tubulin carboxypeptidase and retyrosination by tubulin tyrosine ligase (Tyr-tubulin ↔ Glu-tubulin) (Raybin and Flavin, 1975; Thompson et al., 1979; Gundersen et al., 1984; Wehland and Weber, 1987*a*,*b*). The second modification is irreversible removal either of a second carboxy-terminal amino acid from Glu-tubulin (Glu-tubulin → Δ2-tubulin) or, less likely, of both carboxy-terminal amino acids from Tyr-tubulin (Tyr-tubulin → Δ2-tubulin) (Paturle et al., 1989; Paturle-Lafanechère et al., 1991, 1994). Thus, accumulation of Glu-tubulin, and especially of Δ2-tubulin, in microtubules provides a marker for the age, and hence the stability, of these polymers (Barra et al., 1973; Borisy et al.,

Address correspondence to George Cooper IV, M.D., Cardiology Section, VA Medical Center, 109 Bee Street, Charleston, SC 29401-5799. Tel.: (803) 577-5011, ext. 6858. Fax: (803) 953-6473. E-mail: george_cooper@smtpgw.musc.edu

1. *Abbreviations used in this paper*: EF-1α, translation elongation factor-1α; LV, left ventricle; MAP 4, microtubule-associated protein 4; RV, right ventricle.

© The Rockefeller University Press, 0021-9525/97/11/963/11 $2.00

1975; Bulinski and Gundersen, 1991). To exploit these markers of microtubule stability, we prepared antibodies for Tyr-, Glu-, and Δ2-tubulin and examined the prevalence of each in the microtubules of cardiocytes and in the total protein of myocardium from normally loaded control and pressure overload-hypertrophied ventricles.

If this hypothesis were found to be valid, three potential explanations for increased microtubule stability, which center on microtubule regulatory proteins, seemed most plausible: first, an increased number of polymer nucleating microtubule organizing centers, and thus of their constituent γ-tubulin (Joshi et al., 1992); second, a decrease in translation elongation factor-1α (EF-1α), which has microtubule severing activity (Shiina et al., 1994); and third, an increase in the predominant cardiac microtubule-associated protein, MAP 4, which binds to and thereby may stabilize microtubules (Bulinski and Borisy, 1979, 1980). We addressed this question as well by generating antibodies to these three microtubule regulatory proteins.

Materials and Methods

Experimental Models

Long-term RV pressure overload hypertrophy was induced by partially occluding the pulmonary artery of cats with a 3.2-mm internal diameter band, just as we have described before (Cooper et al., 1973*b*). These cats were allowed to recover for 1 d to 6 mo. Short-term RV pressure overload was induced as before (Rozich et al., 1995) by partial occlusion of the pulmonary artery with a balloon-tipped cathether. In these cats, RV pressure was doubled for 1 or 4 h. Long-term volume overload RV hypertrophy was induced by resecting the interatrial septum during venous inflow occlusion, again as described before (Cooper et al., 1973*a*). These cats were allowed to recover for 2 or 4 wk. Controls consisted of sham-operated cats submitted to thoracotomy and pericardiotomy without hemodynamic intervention. In all cases, the left ventricle (LV) served as a same-animal normally loaded control. All operative procedures were carried out under full surgical anesthesia with meperidine (2.2 mg/kg i.m.), ketamine HCl (50 mg/kg i.m.), and acepromazine maleate (0.25 mg/kg i.m.). All procedures and the care of the cats were in accordance with institutional guidelines.

Hemodynamic Status

At terminal study, the control cats, the long-term pressure overload cats, and the long-term volume overload cats were anesthetized as above. Right heart and systemic arterial pressures were obtained as before (Tsutsui et al., 1994). The arterio-venous difference in oxygen content was used as a measure of the adequacy of systemic perfusion, and in the volume overload cats the difference in percent oxygen saturation of hemoglobin between the right atrium and the superior vena cava was used as the indication of a left-to-right shunt at the atrial level. The short-term pressure overload cats were anesthetized with meperidine (10 mg/kg i.m.), followed after 15 min by methohexital sodium (20 mg/kg i.p.), and followed after a further 15 min by α-chloralose (60 mg/kg i.v.).

Cardiocyte Isolation

The enzymatic perfusion method that we use to obtain reproducible yields of calcium-tolerant, quiescent cardiocytes from the RV and LV of cats has been described in our previous work (Cooper et al., 1986; Mann et al., 1989, 1991; Kent et al., 1989). After obtaining the RV and LV weights, cardiocytes were isolated separately from each ventricle and maintained for 1 h before further usage at 37°C in 1.8 mM Ca^{2+} mitogen-free M-199 medium at pH 7.4.

Posttranslationally Modified α-Tubulin

Antibodies. Antibodies against native α-tubulin and two posttranslationally modified forms of α-tubulin were prepared by the method of Gundersen et al. (1984). The sequences of the peptide immunogens were: EEEGEEY (the carboxy-terminal amino acid sequence of native Tyr-tubulin), GEEEGEE (the carboxy-terminal amino acid sequence of Glu-tubulin), and EGEEEGE (the carboxy-terminal amino acid sequence of Δ2-tubulin). These peptides were KLH-conjugated by cross-linking with glutaraldehyde and injected into rabbits. Sera were monitored for antibody activity on slot blots using BSA-conjugated peptides. Antibody specificity was validated by immunoblotts of purified Tyr-, Glu-, and Δ2-tubulin isoforms, a gift from L. Paturle-Lafanechère (Centre d'Etudes Nucleaires de Grenoble, France).

Myocardial Homogenates. After completion of the hemodynamic studies, the cats were heparinized (1,000 units i.v.) and placed on oxygen. A midline thoracotomy was performed, the pericardium opened, and the heart rapidly removed and weighed. The aorta was then cannulated, and the coronary arteries were gently flushed with microtubule stabilization buffer (Ostlund et al., 1979). Two 0.25-gm specimens were then excised both from the RV and LV free walls for tubulin protein isolation. The remaining myocardium was immediately rinsed in ice-cold saline, after which additional tissue from the RV and the LV free walls was excised and flash-frozen in liquid nitrogen for RNA isolation. For immunoblot analysis, 0.25-gm RV and LV specimens were homogenized in 5 ml of the microtubule stabilization buffer and centrifuged at 100,000 *g*, 25°C for 15 min. The supernatants were saved as the free tubulin fractions, and the pellets were resuspended at 0°C in 4 ml of microtubule depolymerization buffer (Schliwa et al., 1981); after 1 h at 0°C they were centrifuged at 100,000 *g*, 4°C for 15 min, and the supernatants were saved as the polymerized tubulin fractions. The remaining 0.25-gm RV and LV specimens were homogenized in 5 ml of microtubule depolymerization buffer, maintained for 1 h at 0°C, and centrifuged at 100,000 *g*, 4°C for 15 min. These supernatants were saved as the total tubulin fractions. Protease and phosphatase inhibitors were used throughout.

Immunoblots. For the subsequent 12.5% SDS-PAGE, equal proportions of free, polymerized, and total tubulin samples were loaded onto the three lanes for each ventricle, and an equal amount of protein as determined by a bicinchoninic acid assay (BCA; Pierce Chem. Co., Rockford, IL) was loaded for the RV and LV samples. The samples were transferred to polyvinylidene difluoride membranes (500 mA, 120 min, 4°C) and probed with a 1:5,000 dilution of a mAb to α-tubulin (DM1A; Amersham Corp., Arlington Heights, IL) or β-tubulin (DM1B; Amersham Corp.), or with the Tyr-, Glu-, and Δ2-tubulin antibodies which we had generated. Bound antibody was visualized using a horseradish peroxidase-conjugated secondary antibody (Vector Laboratories, Burlington, CA) and enhanced chemiluminescence (ECL; Amersham Corp.). In all cases, a single 55-kD band having the same mobility as concurrently run bovine brain β-tubulin was detected. Densitometric quantification of the immunoblots was carried out as described before (Tsutsui et al., 1994).

This analysis of the free, polymerized, and total tubulin fractions was validated in five cats by densitometry of blots probed with the β-tubulin antibody. The sum of the free and polymerized tubulin fractions was 89.0 ± 0.6% of the total tubulin fraction. When in these samples the residual pellet of the second centrifugation was boiled in SDS and immunoblotted, the β-tubulin was only 2.2 ± 1.5% of that in the polymerized tubulin fraction, and when the pellet containing the polymerized fraction was washed with microtubule stabilization buffer, the free tubulin that had carried over into the polymerized tubulin fraction was only 1.6 ± 0.7% of that in the polymerized tubulin fraction. Thus, the separation and measurement of the three tubulin fractions was satisfactory.

Indirect Immunofluorescence Micrographs. For visualization of the appearance and density of the cardiocyte microtubule network, freshly isolated RV and LV cardiocytes were sedimented onto laminin-coated coverslips at 1 *g* for 45 min, extracted for 1 min in 1% Triton X-100 (Sigma Chemical Co., St. Louis, MO) in the microtubule stabilization buffer, washed 3 times in the same buffer, and fixed for 30 min with 3.7% formaldehyde, all at 25°C. After blocking with 10% donkey serum in 0.1 M glycine, the cells were incubated overnight at 4°C with a 1:50 dilution of the same antibodies used for the immunoblots, followed by a fluorescein-conjugated secondary antibody (Jackson ImmunoResearch Laboratories, West Grove, PA); 0.7-μm optical sections were then acquired by confocal laser microscopy (LSM GB-200; Olympus Optical Co., Ltd., Tokyo, Japan).

Taxol Usage. To determine in normal cardiocytes whether the α-tubulin of stablized microtubules exhibits time-dependent posttranslational modifications, 10^{-5} M taxol, which inhibits microtubule depolymerization, was added to a chamber containing freshly isolated cardiocytes, which were sampled for immunofluorescence microscopy of native and posttranslationally modified α-tubulins after 0.0, 0.5, 1.0, and 2.0 h.

Microtubule Stability

Nocodazole. The prevalence of posttranslationally modified α-tubulin in cardiocyte microtubules was used as the primary measure of the age, and thus the intrinsic stability, of these polymers. Resistance to nocodazole-induced microtubule depolymerization was used as one of two additional measures of microtubule stability. For this purpose, freshly isolated cardiocytes were sedimented onto laminin-coated coverslips at 1 *g* for 45 min, washed twice with 0.3 μM nocodazole (Aldrich Chemical Co., Milwaukee, WI) in PBS, exposed to 0.3 μM nocodazole in M-199 medium for 0.0, 0.5, 1.0, or 1.5 h, extracted for 1 min in 1% Triton X-100 (Sigma) in the microtubule-stabilizing buffer, all at 25°C, and prepared as above for indirect immunofluorescence confocal microscopy using the antibody to β-tubulin (DM1B; Amersham).

Low Temperature. The rate of microtubule depolymerization at 0°C was used as the second additional measure of microtubule stability. For this purpose, freshly isolated cardiocytes were sedimented onto laminin-coated coverslips at 1 *g* for 45 min and then immersed in 0°C M-199 medium for 0.0 or 1.0 h, extracted for 1 min in 1% Triton X-100 (Sigma) in the microtubule-stabilizing buffer, and prepared as above for indirect immunofluorescence confocal microscopy using the antibody to β-tubulin (DM1B; Amersham).

Microtubule Regulatory Proteins

γ-Tubulin. An antibody against γ-tubulin was prepared as described (Joshi et al., 1992). The sequence selected for the peptide immunogen was: EEFATEGTDRKDVFFY (residues 38–53 of human γ-tubulin), since, except for two amino acids, this sequence is conserved from yeast through human. This peptide was KLH-conjugated by cross-linking with glutaraldehyde and injected into rabbits. The serum was monitored for antibody activity on slot blots using BSA conjugated to the peptide. IgG was purified from whole antiserum by chromatography on a protein A/G column (Pierce). Antibody specificity was validated by immunoblot analysis using an extract from non-cardiocyte (interstitial and vascular) cells obtained from feline hearts. For preparation of the noncardiocyte cell extract, cells which adhered to a culture flask after enzymatic digestion of the feline heart were cultured for 4 d in DMEM with 5% fetal calf serum. After removal of the medium, the cell extract was prepared by solubilizing the cells directly in a buffer consisting of 10 mM Tris, pH 6.8, and 1% SDS. The protein concentration of each extract was determined by a bicinchoninic acid assay (BCA; Pierce).

For immunofluorescent localization of γ-tubulin in noncardiocytes, cells cultured on coverslips were fixed by plunging them into –20°C methanol for 5 min. The coverslips were air-dried, rehydrated in PBS, blocked with 10% donkey serum in 0.1 M glycine, and incubated overnight at 4°C with 1:50 dilutions of antibodies to β-tubulin and γ-tubulin. Fluorescein-conjugated anti-rabbit IgG and Cy3-labeled anti–mouse IgG (Jackson ImmunoResearch Laboratories) were used as secondary antibodies. For immunofluorescent localization of γ-tubulin in feline cardiocytes, cells on coverslips were fixed in methanol and stained as above.

Elongation Factor-1α. The prevalence of EF-1α in the RVs and LVs both of control cats and of cats with RV pressure overloading was estimated from immunoblots. Total tubulin samples prepared as described above were loaded on 12.5% SDS-PAGE gels, and EF-1α was detected with a polyclonal EF-1α antibody (Shiina et al., 1994), a gift from E. Nishida (Kyoto University, Japan).

Microtubule-associated Protein 4. Free, polymerized, and total tubulin samples, prepared as described above, were used for immunoblot estimation of MAP 4 protein levels in these fractions. The samples were loaded on 7.5 or 12.5% SDS-PAGE gels; microtubule-associated proteins were detected by antibodies to MAP 1, MAP 2, and tau (ICN Pharmaceuticals, Inc., Costa Mesa, CA), as well as MAP 4; the latter was a gift from H. Murofushi (Tokyo University, Japan). Neither MAP 1, MAP 2, nor tau was detected in immunoblots of control or RV pressure overloaded myocardium. Changes in MAP 4 were examined in the RVs and LVs both of control cats and of cats with RV pressure overloading at 2 d and at 1, 2, 4, and 8 wk after pulmonary artery banding.

Because the MAP 4 antibody was raised against bovine MAP 4 (Kotani et al., 1988; Aizawa et al., 1991), we first ascertained its reactivity with MAP 4 from other species, i.e., cat and human, using feline noncardiocyte myocardial cells and human A431 cells grown in serum. These mitotically competent cells would be expected to exhibit MAP 4 staining of the mitotic spindle when dividing. For immunofluorescent localization of cardiocyte MAP 4, freshly isolated feline cardiocytes sedimented onto laminin-coated coverslips were fixed by plunging them into −20°C methanol for 5 min. The coverslips were air-dried, rehydrated in PBS, and post-fixed with 3.7% formaldehyde in PBS for 30 min. They were blocked with 10% donkey serum in 0.1 M glycine and incubated overnight at 4°C with 1:50 dilutions of the monoclonal antibody to β-tubulin and the MAP 4 antibody. Fluorescein-conjugated anti-rabbit IgG and Cy3-labeled anti-mouse IgG (Jackson ImmunoResearch Laboratories) were used as secondary antibodies.

To estimate MAP 4 mRNA levels, poly(A)$^+$ RNA was extracted from frozen cardiac samples (FastTrack II; Invitrogen Corp., San Diego, CA). To load equal amounts of poly(A)$^+$ RNA on each lane of Northern blots, the amount of 3′-UMP in each sample was measured as before (Tagawa et al., 1996) via high pressure liquid chromatography, and 2 μg of poly(A)$^+$ RNA loaded on each lane was electrophoresed on denaturing 2% formaldehyde/1% agarose gels, followed by 2 h of pressure-driven blotting to a nylon membrane (Hybond-N; Amersham Corp.). The RNA was then immobilized on the nylon membrane by UV cross-linking (Stratalinker; Stratagene, La Jolla, CA). The nylon membrane was pre-hybridized for 4 h at 42°C in a solution containing 50% (vol/vol) deionized formamide, 0.2% (wt/vol) Ficoll, 0.02% (wt/vol) polyvinylpyrrolidone, 5× SSC, 10 mM MOPS, pH 7.0, 2 mM EDTA, 100 μg/ml denatured salmon sperm DNA, and 0.2% (wt/vol) SDS. The membrane was hybridized for 16 h at 42°C in a solution containing ^{32}P-radiolabeled probe ($5.0 - 10.0 \times 10^6$ cpm/ml). The Northern blots were washed three times in 2× SSC, 0.1% SDS for 1.5 h at 40°C, followed by a wash in 0.2× SSC, 0.1% SDS for 0.5 h at 42°C, and then processed for autoradiography.

Three PCR-generated probes were prepared for MAP 4 Northern blots. These were 313- and 288-bp probes corresponding to nucleotides 2807–3120 and 3275–3563, respectively, of the murine MAP 4 cDNA sequence (West et al., 1991) and a 223-bp probe corresponding to nucleotides 1925–2148 of the bovine MAP 4 cDNA sequence (Aizawa et al., 1990). The murine MAP 4 cDNA was a gift from J. Olmsted (University of Rochester, NY). Each blot was normalized as before with a GAPDH probe PCR-generated from feline GAPDH cDNA (McDermott et al., 1991).

Data Analysis

The mean value and the standard error of the mean are shown for each group of data. For the data in the table, group means were first compared by a one-way ANOVA, and if a difference was found, then each experimental mean was compared with that of the control and any other groups noted by the appropriate post-hoc test as specified.

Results

Characteristics of the Experimental Models

The goal of the present study was to examine both microtubule stability and its regulation from the earliest stages of RV pressure or volume overload hypertrophy induction, through completion of the hypertrophic growth phase, and then into an extended period of stable hypertrophy. For pressure overload hypertrophy, the pulmonary artery balloon catheter cats were used as the model for early hypertrophy induction (1–4 h), and pulmonary artery banding was used as the model both for the later time points of active hypertrophic growth at 1 d, 2 d, 1 wk, and 2 wk after banding and for the further time points of 1, 2, and 6 mo after banding when the mass of the hypertrophied RV is at a new steady state (Tagawa et al., 1996).

The short-term pulmonary artery balloon catheter cats exhibited a doubling of RV systolic pressure without a significant change in RV end-diastolic pressure. The major features of the long-term surgical models used in this study are summarized in Table I. As shown there, in the long-term pressure overload pulmonary artery banding group, RV systolic pressure was increased more than twofold, while in the long-term volume overload atrial septal defect group, there was a substantial shunt at the atrial level. For both groups, the ratios of RV weight to body weight and

Table I. Characteristics of the Models

	Control (n = 12)	ASD (n = 6)	PAB (n = 24)
RV Systolic Pressure (mmHg)	26.1 ± 1.1	29.4 ± 1.3	55.9 ± 1.5*‡
ΔO_2% Saturation (SVC vs. RA)	0.7 ± 0.3	9.9 ± 1.9*	0.5 ± 0.3‡
RV weight/body weight (g/kg)	0.58 ± 0.04	0.86 ± 0.06*	0.92 ± 0.04*
RV weight/tibal length (g/cm)	0.16 ± 0.01	0.22 ± 0.03*	0.21 ± 0.01*
LV weight/body weight (g/kg)	2.05 ± 0.06	1.97 ± 0.15	2.20 ± 0.07
Body weight (kg)	3.7 ± 0.2	3.6 ± 0.5	3.4 ± 0.1
Arteriovenous O_2 difference (ml/liter)	35.7 ± 3.1	—	38.0 ± 1.4
RV end-diastolic pressure (mmHg)	2.3 ± 0.6	1.6 ± 0.6	2.5 ± 0.5
Liver weight/body weight (g/kg)	26.8 ± 1.1	25.1 ± 0.6	28.9 ± 1.0

Values are mean ±SEM. ASD, atrial septal defect; PAB, pulmonary artery band; SVC, superior vena cava; RA, right atrium. Statistical comparisons are by one-way analysis of variance followed by Neuman-Keuls t test. For the ASD and PAB cats, there was no within-group difference for any of these variables at the different experimental time points; the within-group data are therefore grouped together.
*$P < 0.01$ for difference from control.
‡$P < 0.01$ for difference from ASD.

tibial length were increased significantly and comparably. Body weight was similar in each group, and the ratio of LV weight to body weight did not differ among the groups, precluding any effect of postoperative changes in body weight. In neither group was there evidence for right heart failure in terms of either the presence of ascites and pleural effusion in any cat at the time of study or increases in A-V O_2 difference, RV end-diastolic pressure, or the ratio of liver weight to body weight.

Microtubule Stability in Feline Cardiocytes

Specificity of Antibodies to Posttranslationally Modified α-Tubulin. *B*ecause the specificity of our Tyr-, Glu-, and Δ2-tubulin antibodies was critically important to the validity of this study, a 100-ng aliquot of each purified α-tubulin protein isoform was loaded on an SDS-PAGE gel, blotted, and probed with all three antibodies. The Tyr-tubulin antibody showed no cross-reactivity with either Glu-tubulin or Δ2-tubulin (Fig. 1 *A*). The Glu-tubulin antibody showed only very minor cross-reactivity with Tyr-tubulin and none with Δ2-tubulin (Fig. 1 *B*), and the Δ2-tubulin antibody showed only minor cross-reactivity with Glu-tubulin (Fig. 1 *C*). Of note, cross-reactivity of any degree was not observed when tubulin isoform quantities ⩽50 ng were loaded, an amount commensurate with the maximum loading employed herein for the semiquantitative analysis of posttranslationally modified α-tubulin isoforms.

Posttranslationally Modified α-Tubulin in Control Cardiocytes. To determine whether the presence of posttranslationally modified α-tubulin isoforms is a valid index of cardiocyte microtubule age, we exposed normal cardiocytes to taxol. This diterpene binds to microtubules and prevents their depolymerization, such that the life-time of the microtubules increases. Initially, as seen in the three panels *A* in Fig. 2, the density of the microtubule network

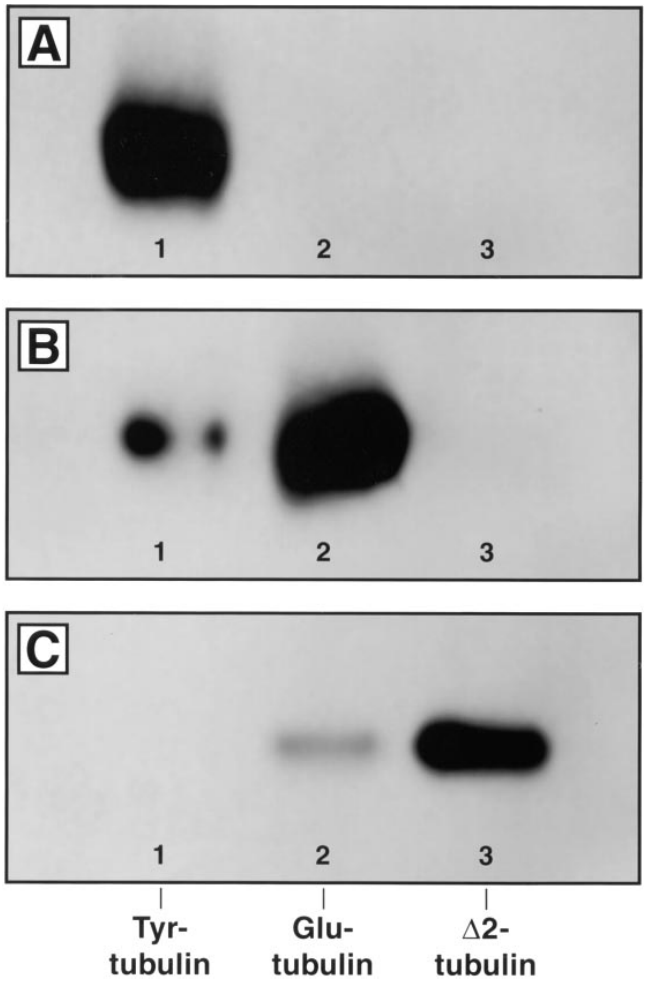

Figure 1. Specificity of the antibodies to posttranslationally modified isoforms of α-tubulin. Immunoblot analysis. A 100-ng sample of a single α-tubulin isoform was loaded on each lane before 12.5% SDS-PAGE, where lane *1*, Tyr-tubulin; lane *2*, Glu-tubulin; and lane *3*, Δ2-tubulin. The blot in *A* was then probed with anti–Tyr-tubulin antibody, the blot in *B* was probed with anti–Glu-tubulin antibody, and the blot in *C* was probed with anti–Δ2-tubulin antibody.

stained with the Tyr-tubulin antibody was similar to that in normal cells stained with the β-tubulin antibody (Tsutsui et al., 1993); however, microtubule staining with the Glu-tubulin and Δ2-tubulin antibodies was virtually absent. At 30 min of taxol exposure, as seen in the three panels *B* in Fig. 2, there was a modest increase in the density of the microtubule array stained with the Tyr-tubulin antibody, and microtubule decoration with the Glu-tubulin and Δ2-tubulin antibodies, which as in differentiating myoblasts (Gundersen et al., 1989) is punctate rather than uniform, was just becoming apparent. At both 60 and 120 min of taxol exposure, as seen in the three panels *C* and *D*, respectively, in Fig. 2, the density of the microtubule array stained with the Tyr-tubulin antibody increased further coincident with continuing microtubule assembly; however, the density of the microtubule arrays stained with the Glu-tubulin and Δ2-tubulin antibodies increased quite remarkably, as the duration of taxol exposure increased, and their constituent α-tubulin underwent progressive post-

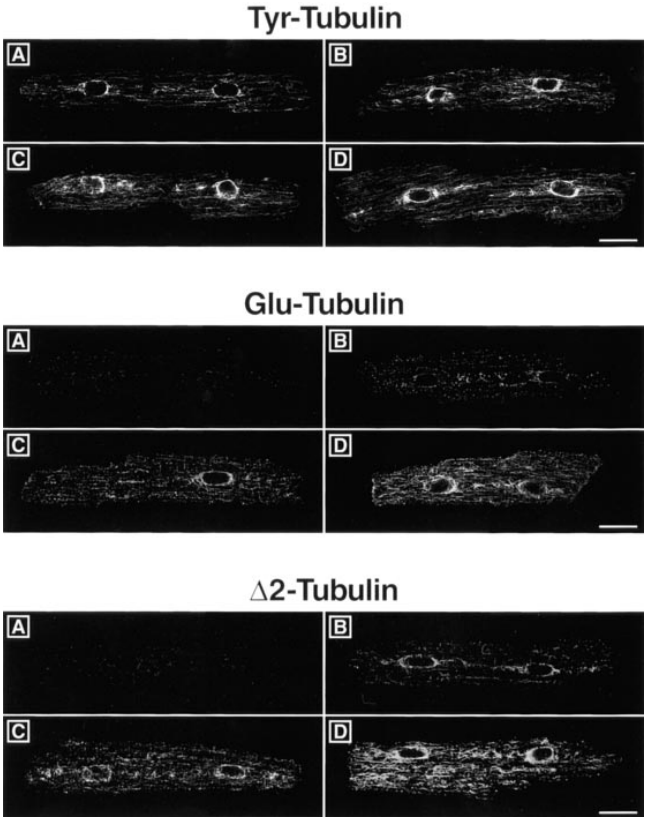

Figure 2. Taxol-induced microtubule stabilization in normal cardiocytes. Immunofluorescence confocal micrographs of posttranslationally modified α-tubulin isoforms in the microtubules of cardiocytes from a normal feline heart after exposure to 10^{-5} M taxol for 0 (*A*), 0.5 (*B*), 1.0 (*C*), and 2.0 h (*D*). As indicated, the antibodies employed were, from above down, anti–Tyr-tubulin antibody, anti–Glu-tubulin antibody, and anti–Δ2-tubulin antibody. Each micrograph is a single 0.7-μm confocal section taken at the level of the nuclei. Double-staining of cells exposed to taxol for 2 h both with the β-tubulin antibody and with either the Tyr-tubulin, Glu-tubulin, or Δ2-tubulin antibodies showed that the latter three antibodies decorated microtubules exclusively (data not shown). Bar, 25 μm.

translational modification. Thus, successive posttranslational modifications of microtubule-assembled α-tubulin are a valid index of microtubule life-time in normal cardiocytes.

Microtubule Stability in Pressure Overload Hypertrophy. The presence and quantity of posttranslationally modified α-tubulin was then used to estimate microtubule stability in cardiocytes from the hearts of cats with RV pressure overload hypertrophy. In one such animal 2 wk after pulmonary artery banding, Fig. 3 *A* shows that the density of Tyr-tubulin-decorated microtubules is greater in the RV than in the LV cardiocyte. Fig. 3, *B* and *C* shows that the microtubules of the RV but not the LV cardiocytes are decorated by the Glu-tubulin and Δ2-tubulin antibodies. Of interest, double-staining of hypertrophied RV cardiocytes with both Glu-tubulin and Δ2-tubulin antibodies showed coincident decoration of microtubules with both antibodies (data not shown), such that a given microtubule contained both posttranslationally modified forms of α-tubulin. Findings similar to those in Fig. 3 obtained at 2 d, 1 wk, 1 mo, 2 mo, and 6 mo after pulmonary artery banding (data not shown), such that cardiocyte microtubule stabilization occurs early after RV pressure overloading and persists indefinitely thereafter. Indeed, the posttranslationally modified α-tubulin isoforms are appreciable in cardiocyte microtubules even before increased density of the microtubule network is apparent, since this latter phenomenon is not clearly discernible until at least 1 wk after RV pressure overloading (Tagawa et al., 1996).

A quantitative estimate of the extent of microtubule stabilization in pressure-hypertrophied myocardium is provided in Fig. 4, which shows that, when assayed by the isoform nonselective β-tubulin antibody, there is a near doubling of microtubule protein in the pressure-hypertrophied RV; the Tyr-tubulin data show that this does not involve a disproportionate increase in newly formed microtubules. The Glu-tubulin and Tyr-tubulin data, however, show that there is a large and quite disproportionate increase in long-lived, stable microtubules in which posttranslational modifications of α-tubulin have occurred in the hypertrophied RVs. As was the case for the data in Fig. 3, these findings at 2 wk after pulmonary artery banding were confirmed at 2 d, 1 wk, 1 mo, 2 mo, and 6 mo after pulmonary artery banding (data not shown). Thus, the increased cardiocyte microtubule density seen in pressure overload cardiac hypertrophy results not only from new microtubule formation, but also from stabilization of these microtubules once formed.

While the presence of posttranslationally modified α-tubulin isoforms is an index of the age, and thus the intrinsic stability, of the cellular microtubule array under native conditions that obtained in vivo, the resistance of microtubules to depolymerization either by microtubule poisons or by low temperature is another commonly employed measure of microtubule stability for isolated cells in vitro. Fig. 5 shows that the resistance of the microtubule array to depolymerization by either of these modalities is considerably greater in hypertrophied RV than in control LV cardiocytes at 2 wk after RV pressure overloading. Note that while the initial density of the RV cardiocyte microtubule array was greater than that of the LV cardiocyte (Fig. 5, *A* vs. *B* and *I* vs. *J*), the relative difference in densities was far more pronounced at the end point of each treatment (Fig. 5, *G* vs. *H* and *K* vs. *L*). Further, the residual microtubules became much more fragmented in the LV as opposed to the RV cardiocytes during exposure to either nocodazole or low temperature. At 2 d after banding these changes were not discernable, while at 1 wk after banding these changes were present, albeit considerably less marked than those shown in Fig. 5, probably reflecting a gradual accumulation of stable microtubules (data not shown). Thus, these data, which were replicated in a second experimental animal at 2 wk after pulmonary artery banding, confirm through an independent means those data obtained from characterization of posttranslationally modified α-tubulin isoforms.

Microtubule Stability in Volume Overload Hypertrophy. To determine whether increased microtubule stability is a generalized property of hypertrophied cardiocytes or is instead specific to the type of hemodynamic overload causative of the hypertrophy, we generated an equivalent degree of feline RV hypertrophy in response to a volume

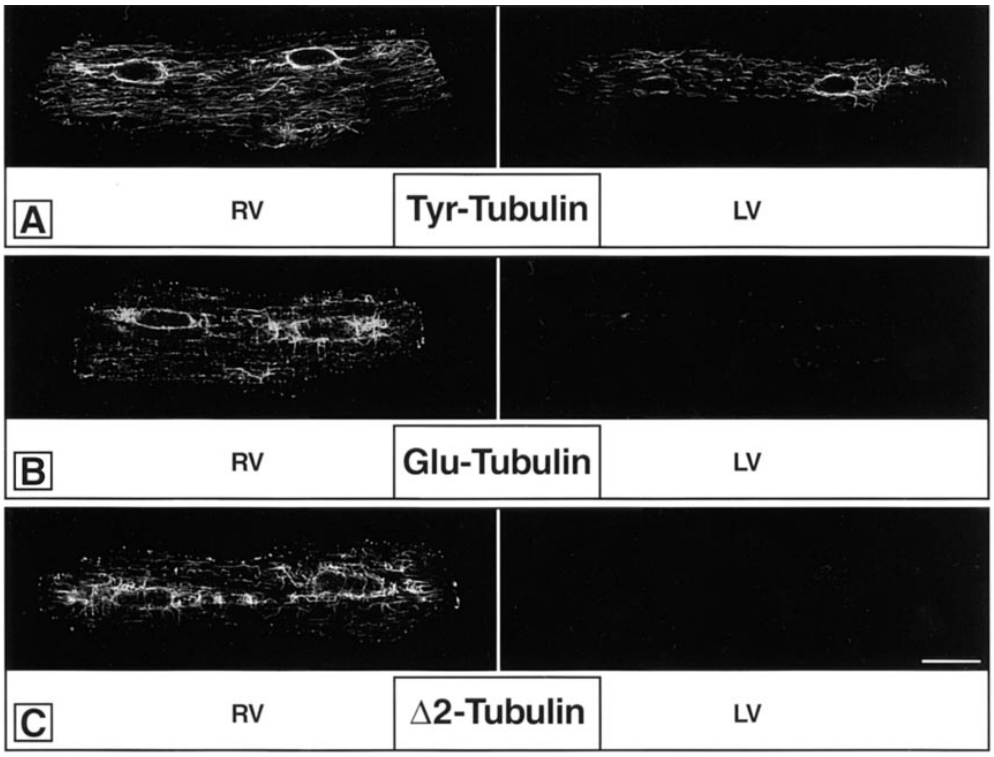

Figure 3. Microtubule stability in pressure overload-hypertrophied myocardium: Immunofluorescence confocal micrographs of posttranslationally modified α-tubulin isoforms in RV and LV cardiocyte microtubules from a feline heart 2 wk after RV pressure overloading. The anti–Tyr-tubulin antibody was used in *A*, the anti–Glu-tubulin antibody was used in *B*, and the anti–Δ2-tubulin antibody was used in *C*. Each micrograph is a single 0.7-μm confocal section taken at the level of the nuclei. Bar, 25 μm.

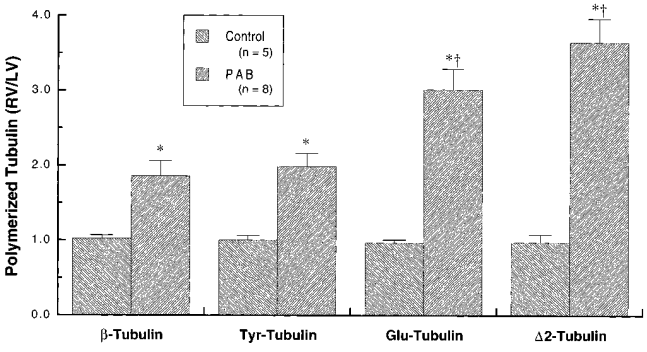

Figure 4. Densitometric analysis of microtubule stability in pressure overload-hypertrophied myocardium. β-tubulin and posttranslationally modified α-tubulin isoforms in microtubules of RVs and LVs from the same feline hearts. Control cats were compared with cats RV pressure overloaded 2 wk earlier via pulmonary artery banding. Four blots were prepared for each heart; the microtubule fractions from the RV and LV (20 μg protein/lane) were loaded on two lanes, and four concentrations of the appropriate protein standard (7.5–60.0 ng/lane) were loaded on the remaining lanes before 12.5% SDS-PAGE; the blot was then probed with the corresponding antibody. For the protein standards, the linear relationship between optical density and protein loaded had a correlation coefficient ⩾0.98 in each instance. Of the total α-tubulin, Tyr-tubulin comprised 92.6 ± 2.1%, Glu-tubulin was 4.6 ± 1.4%, and Δ2-tubulin was 2.8 ± 0.7%. Statistical comparisons were by one-way ANOVA followed by Scheffé's S procedure, where n = number of cats in each group.*$P < 0.01$ for difference within a category from the control group value by Scheffé's S procedure. ‡$P < 0.01$ for difference from the β-tubulin and Tyr-tubulin values within the hypertrophy group by Scheffé's S procedure.

overload as we had generated in response to a pressure overload. In one such animal 2 wk after atrial septotomy, Fig. 6 *A* shows first that the density of the microtubule network decorated by the antibody specific for native Tyr-tubulin is less in this volume-hypertrophied RV cardiocyte than that seen in the pressure-hypertrophied RV cardiocyte (Fig. 3 *A*). Second, *B* and *C* of Fig. 6 show that posttranslationally modified α-tubulin isoforms are virtually absent in these cardiocytes, just as they are in normally loaded LV cardiocytes from the RV pressure-overloaded hearts (Fig. 3). These findings, which were confirmed by immunoblots, were replicated at 4 wk after atrial septotomy (data not shown). Thus, an equivalent degree and duration of RV hypertrophy in response to a volume overload as that seen in response to a pressure overload results neither in cardiocyte contractile dysfunction (Tsutsui et al., 1993) nor in increased density or stability of the cardiocyte microtubule network.

Microtubule Regulatory Proteins

γ-Tubulin. When the anti–γ-tubulin antibody that we prepared was used to probe extracts from non-cardiocytes and cardiocytes from a normal feline heart, a clear band at 46 kD was seen for the noncardiocyte extract, but no band was seen for the cardiocyte extract (data not shown), suggesting that γ-tubulin is not present in any appreciable quantity in these cells. Immunofluorescence micrographs confirmed these observations: cardiac fibroblasts showed clear γ-tubulin staining in well-defined microtubule organizing centers; however, cardiocytes showed no γ-tubulin staining, and the same finding obtained in pressure-hyper-

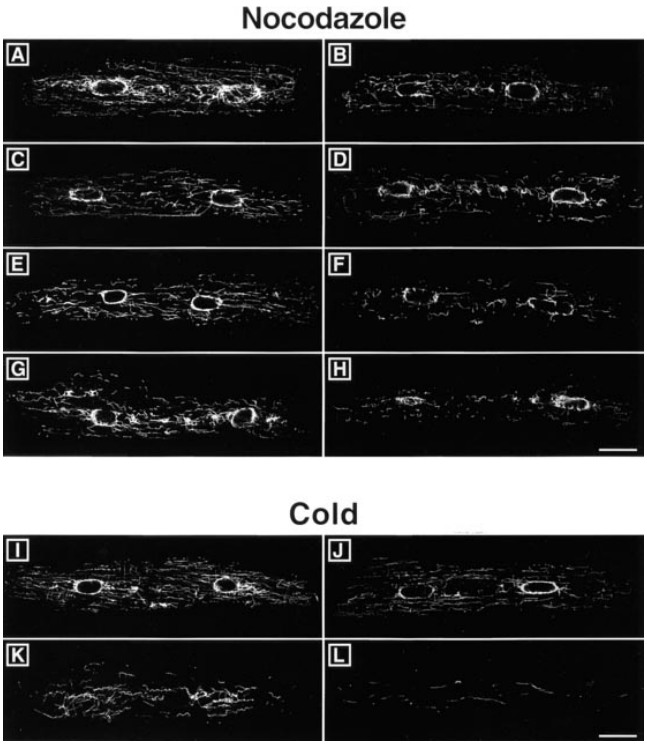

Figure 5. Microtubule stability in pressure overload-hypertrophied myocardium: Immunofluorescence confocal micrographs, using the DM1B anti–β-tubulin antibody, of RV and LV cardiocyte microtubules during exposure to nocodazole (*A–H*) or low temperature (*I–L*). Cardiocytes from a feline heart 2 wk after RV pressure overloading were exposed to 0.3 μM nocodazole for 0 min (*A* and *B*), 30 min (*C* and *D*), 60 min (*E* and *F*), or 90 min (*G* and *H*) or they were exposed to a temperature of 0°C for 0 (*I* and *J*) or 60 min (*K* and *L*) before fixation. The cardiocytes on the left (*A, C, E, G, I,* and *K*) are from the RV, and the cardiocytes on the right (*B, D, F, H, J,* and *L*) are from the LV. Of interest, after 90 min of nocodazole exposure the majority of the residual microtubules of RV but not LV cardiocytes was found by double-staining to be decorated by both the β-tubulin and either the Glu-tubulin or Δ2-tubulin antibodies (data not shown). Each micrograph is a single 0.7-μm confocal section taken at the level of the nuclei. Bar, 25 μm.

trophied cardiocytes (data not shown). Therefore, γ-tubulin–containing microtubule organizing centers, at least within the sensitivity of this measurement, are absent from adult cardiocytes, such that an increased number of these microtubule nucleating sites would appear to be excluded as a cause for the increased cardiocyte microtubule network density characteristic of pressure overload cardiac hypertrophy.

Elongation Factor-1α. Immunoblots of control cat myocardium and of RV myocardium at 0, 1, 2, 14, and 30 d after RV pressure overloading showed both that EF-1α protein concentrations are the same in all animals in the RV and in the LV and that there is no change in EF-1α protein concentration in the hypertrophied RVs (data not shown). Thus, reduced microtubule degradation based on reduced EF-1α content would also appear to be excluded as a cause for the increased cardiocyte microtubule density characteristic of pressure overload cardiac hypertrophy.

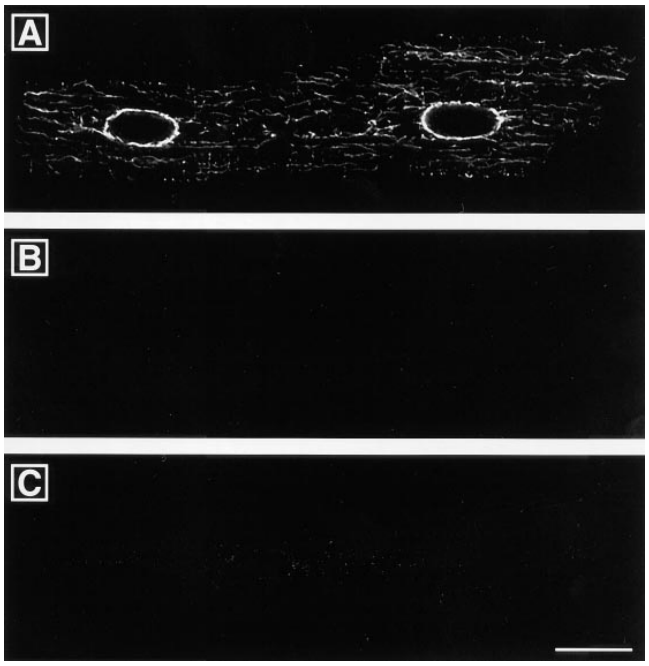

Figure 6. Microtubule stability in volume overload-hypertrophied RV myocardium. Immunofluorescence confocal micrographs of posttranslationally modified α-tubulin isoforms in microtubules of RV cardiocytes from a feline heart 2 wk after RV volume overloading. Anti–Tyr-tubulin antibody was used in *A*, anti–Glu-tubulin antibody was used in *B*, and anti–Δ2-tubulin antibody was used in *C*. Each micrograph is a single 0.7-μm confocal section taken at the level of the nuclei. Bar, 25 μm.

Microtubule-associated Protein 4. Although as noted the MAP 4 antibody which we used was raised against bovine MAP 4 as the immunogen, immunofluorescence staining of human A431 cells and feline cardiac fibroblasts showed strong reactivity with the spindle fibers of dividing cells (data not shown), such that this antibody has significant species cross-reactivity. The immunoblots in *A* (control heart) and *B* (2 wk pulmonary artery banded heart) of Fig. 7, for which equal protein loading was employed, show first that most of the MAP 4 is, as expected, located in the microtubule fraction (the total tubulin fraction in lanes *5* and *6* includes both free and polymerized tubulin) and second that there is a marked increase in MAP 4 protein in the pressure-hypertrophied RV myocardium; no bands other than those shown in this figure were apparent in these immunoblots. The micrographs in *C* and *D* of Fig. 7 are confirmatory: the minimal MAP 4 staining of the control cardiocyte is not well localized to the microtubules, while the hypertrophied cardiocyte shows strong MAP 4 staining, with coincident decoration of the dense microtubule network both with the anti–β-tubulin antibody and with the anti–MAP 4 antibody. This latter finding was confirmed in further RV and LV cardiocytes at 2 d, 1 wk, 1 mo, and 2 mo after RV pressure overloading. Thus, in the evanescent microtubules of normal cardiocytes, very little of the relatively small MAP 4 pool is decorating the microtubules, while the long-lived microtubules of the hypertrophied cardiocytes are binding a significant fraction of a markedly increased pool of MAP 4 protein.

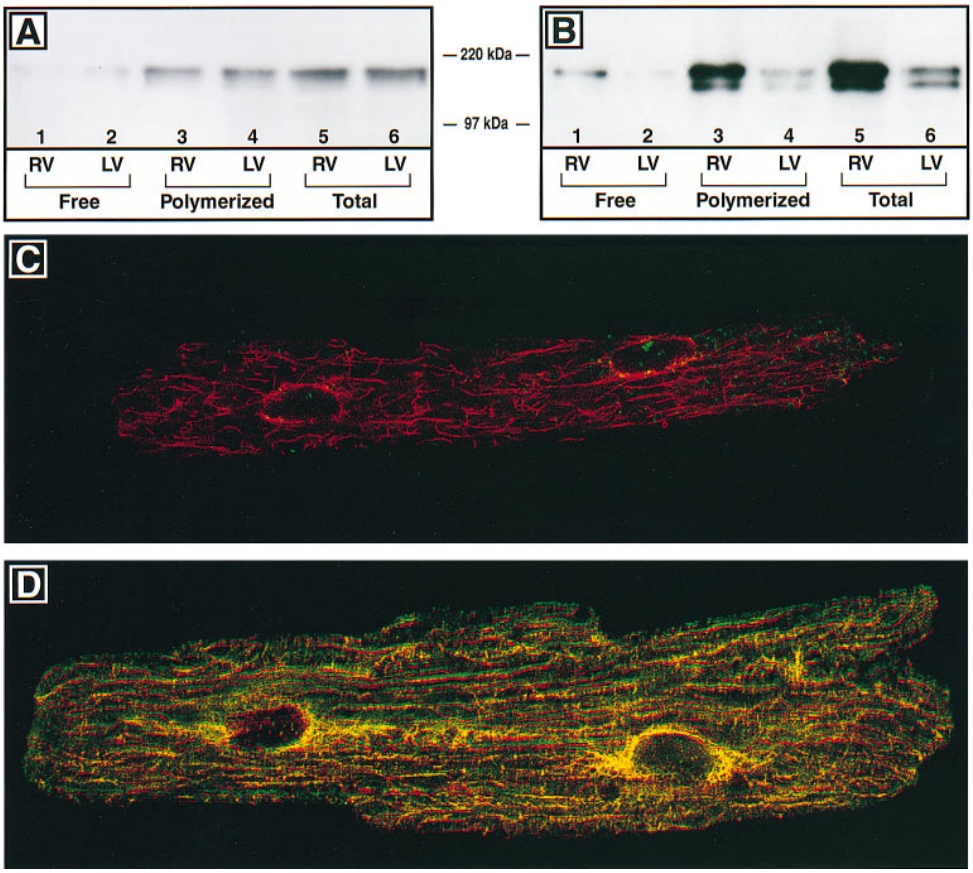

Figure 7. MAP 4 protein in pressure overload-hypertrophied RV and control LV myocardium. Immunoblot and immunofluorescence confocal micrographic analysis of MAP 4. The immunoblot in *A* was prepared from a normal feline heart, and the immunoblot in *B* was prepared from a feline heart 2 wk after RV pressure overloading. For both panels, lanes *1* and *2* were prepared as the free tubulin fraction, lanes *3* and *4* were prepared as the polymerized tubulin fraction, and lanes *5* and *6* were prepared as the total tubulin fraction. Lanes *1*, *3*, and *5* of the immunoblots are from the RV, and lanes *2*, *4*, and *6* of the immunoblots are from the LV. Each blot was probed with anti–MAP 4 antibody. *C* is a micrograph of a cardiocyte from a normal feline heart, and *D* is a micrograph of a RV cardiocyte from a feline heart 2 wk after RV pressure overloading. These cardiocytes were double-stained for β-tubulin (*red*) and MAP 4 (*green*), where the β-tubulin and MAP 4 primary antibodies were followed by species-specific fluorochrome-conjugated secondary antibodies. Each micrograph is a single 0.7-μm confocal section taken at the level of the nuclei.

To gain insight into the potential role of MAP 4 in microtubule stabilization, the relative upregulation on the protein level of β-tubulin and MAP 4 in hypertrophied RV myocardium was examined. Fig. 8 shows that while both β-tubulin and MAP 4 are increased in hypertrophied RV as opposed to normal LV myocardium, the increase in MAP 4 is greater than that in β-tubulin. Indeed, densitometric analysis of immunoblots from 4 cats with RV pressure overload hypertrophy showed that the RV/LV ratio of MAP 4 was threefold greater than the RV/LV ratio of β-tubulin.

Fig. 9 shows the time course of MAP 4 upregulation in pressure overload-hypertrophied myocardium on the mRNA and protein levels. *A* and *B* show that RV MAP 4 mRNA increases substantially by 4 h after pressure loading, whereas β-tubulin and α-tubulin mRNA upregulation is not seen until 1 d after pressure loading (Tagawa et al., 1996), and MAP 4 mRNA remains elevated at least until the hypertrophic growth process is complete 2 wk later. Fig. 9, *C* and *D* show that the resultant increase in RV MAP 4 protein is apparent as early as 2 d after pressure loading and persists indefinitely thereafter.

Thus, the data in Figs. 8 and 9 show that MAP 4 is upregulated both more quickly and more extensively than tubulin after cardiac pressure loading. While this certainly does not establish a cause-and-effect relationship, it does constitute a basis for positing a role for MAP 4 in microtubule stabilization and/or tubulin upregulation.

Discussion

The cardiocyte contractile dysfunction characteristic of pressure overload cardiac hypertrophy is accounted for to a remarkable degree by increased density of the cellular microtubule network (Tsutsui et al., 1993, 1994), which imposes a primarily viscous load on active myofilaments; that is, structural damping via intracellular frictional dissipation that impedes sarcomere shortening (Tagawa et al., 1997). This is accompanied by persistent increases in α- and β-tubulin on both the mRNA and protein levels (Tagawa et al., 1996). Thus, increased synthesis of αβ-tubulin heterodimers, effecting in turn microtubule formation, is one apparent cause for this greater microtubule density. Given, however, that the αβ-tubulin heterodimer–microtubule system is in dynamic equilibrium, enhanced microtubule stability is a second, and potentially synergistic, candidate mechanism for augmented microtubule density. This study was designed to evaluate this second potential mechanism.

The restriction of the two sequential posttranslational

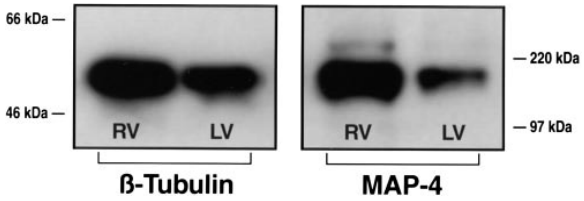

Figure 8. Upregulation of β-tubulin versus MAP 4 protein in pressure overload-hypertrophied myocardium. Immunoblot analysis. The samples for each lane were prepared as the total tubulin fraction, and equal protein loading was employed for the RV and LV samples. For β-tubulin, the DM1B antibody used here recognizes all β-tubulin isoforms. While both β-tubulin and MAP 4 were greater in the hypertrophied RV than in the same-animal normally loaded LV, densitometric analysis of immunoblots from 4 such cats RV pressure overloaded 2 wk earlier via pulmonary artery banding showed that the RV/LV ratio of MAP 4 was 3.0 ± 0.5-fold greater than the RV/LV ratio of β-tubulin.

modifications of α-tubulin solely to microtubule-assembled α-tubulin (Bulinski and Gundersen, 1991; Paturle-Lafanechère et al., 1994) provided an attractively simple and specific strategy for this evaluation. This strategy for estimating microtubule age, which has been applied in other contexts (Schulze and Kirschner, 1987; Webster et al., 1990), has the very conspicuous advantage of not modifying the tubulin–microtubule equilibrium, as must inevitably occur with the usage of tubulin binding agents or the microinjection of fluorochrome-labeled tubulin. Further, in contrast to the situation in nervous tissue and testis, essentially all muscle α-tubulin participates in this cycle of posttranslational modifications (Alonso et al., 1993). Our success in this effort has allowed us to conclude that the microtubules of pressure-hypertrophied cardiocytes do, in fact, demonstrate markedly enhanced stability, wherein microtubule stabilization begins very shortly after cardiac pressure overloading and persists indefinitely thereafter.

We then focused on the basis for this microtubule stabilization. Here, initial insight was provided by the two findings that there is not only a conspicuous increase in microtubules in hypertrophied myocardium, but also a disproportionate increase in stable microtubules (Fig. 4). Further, neither increased microtubule nucleation nor decreased microtubule breakdown appear to be operative mechanisms for the microtubule network densification characteristic of pressure overload cardiac hypertrophy. That is, while microtubule polymerizing and/or depolymerizing mechanisms other than those which we examined could well be effectual, neither is there an increase in microtubule nucleating γ-tubulin nor is there a decrease in microtubule depolymerizing EF-1α. With respect to γ-tubulin, as is the case in neuronal axons (Baas and Joshi, 1992), we found no γ-tubulin–containing microtubule organizing center in the terminally differentiated cardiocyte; this finding is consistent with the known absence of centrosomal microtubule organizing centers from interphase striated muscle cells (Kronebusch and Singer, 1987). Thus, increased microtubule density in hypertrophied cardiocytes is not based on an increased number of the γ-tubulin–containing microtubule organizing centers ordinarily responsible for microtubule nucleation (Archer and Solomon, 1994). With

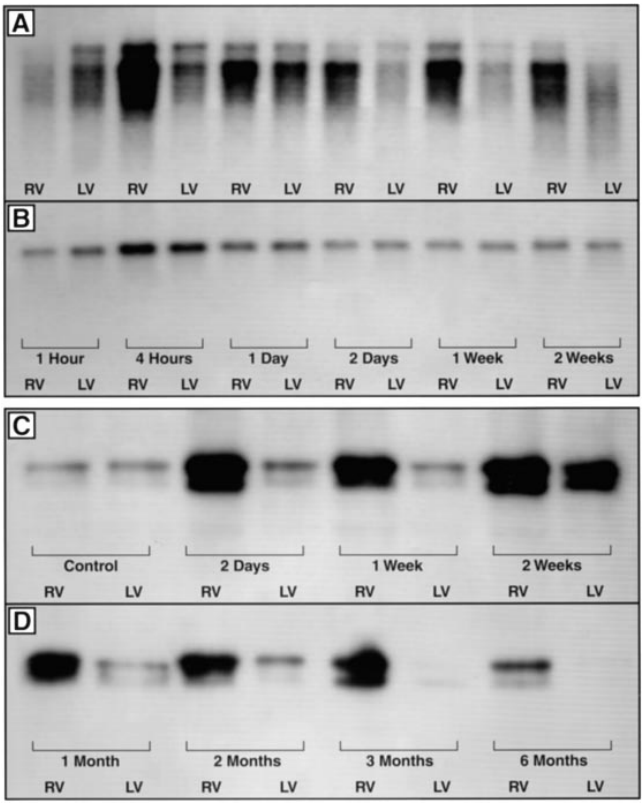

Figure 9. Time course of MAP 4 mRNA and protein upregulation in control LV and pressure overload-hypertrophied RV myocardium. Northern blot and immunoblot analysis. (*A* and *B*) At the indicated times after RV pressure overloading, poly(A)$^+$ RNA was prepared from the RV and LV of each heart, and 1 μg was loaded on each lane. The blot in *A* was probed for MAP 4, and the blot in *B*, which was used to verify equal RV versus LV loading at each time point, was probed for constitutively expressed glyceraldehyde-3-phosphate dehydrogenase. (*C* and *D*) At the indicated times after RV pressure overloading, the total tubulin protein fraction was prepared from the RV and LV of each heart, and 40 μg was loaded on each lane before probing with anti–MAP 4 antibody. Note that the time points chosen for the mRNA and protein blots do not coincide.

respect to EF-1α, the quantity of this protein does not change in the pressure-overloaded RV at any point in the hypertrophy process. Therefore, it is unlikely that reduced EF-1α–based microtubule severing (Shiina et al., 1994, 1995) is causative of increased microtubule density in hypertrophied cardiocytes. Indeed, since the microtubule severing activities of EF-1α, as well as those of katanin (McNally and Vale, 1993) and centrin (Sanders and Salisbury, 1994), tend to be spatially associated with the centrosome and temporally associated with the G_2–M phase transition of the cell cycle, and since the cardiocyte both apparently lacks a classical centrosome and is terminally differentiated, a reduction in endogenous cellular microtubule severing activity would not be expected during cardiac hypertrophy.

Considering, then, the extra-microtubule factor(s) which might stabilize cardiocyte microtubules, MAP 4 was both an obvious candidate in that it is the predominant nonmotor MAP of cardiac muscle (Olmsted, 1986) and a logical

candidate in that its functional role has been thought to be the stabilization of microtubules during the interphase portion of the cell cycle (Bulinski and Borisy, 1979, 1980). Fig. 7 shows that indeed there is a clear increase in MAP 4 protein in the pressure-hypertrophied RV, that this protein is preferentially localized to the microtubule fraction by immunoblotting, and that MAP 4 colocalizes with microtubules micrographically. Fig. 8 shows that this increase in MAP 4 is considerably greater than the increase in tubulin in hypertrophied myocardium. Fig. 9 shows further that MAP 4 mRNA increases as early as 4 h after RV pressure overloading, with this increase persisting throughout the hypertrophy process, while increased MAP 4 protein is seen as early as 2 d after RV pressure overloading, with this increase, as is the case for microtubule densification and microtubule-related cardiocyte contractile dysfunction (Tsutsui et al., 1994), persisting indefinitely thereafter. Of note, MAP 4 upregulation occurs earlier after myocardial pressure loading than does tubulin upregulation (Tagawa et al., 1996). In considering the sequence of these changes, however, one must recognize both that techniques having greatly different sensitivities are being used and that the kinetics of the first appearance of a molecule as reported by a relatively sensitive measure such as Northern or Western blotting may be very different from the kinetics of the accumulation of a macromolecular array as reported by a relatively insensitive measure such as microscopically assessed microtubule density. In this context, it is by no means surprising that MAP 4 is upregulated on the message level at 4 h and then on the protein level at 1–2 d, with the presumably related change in microtubule density only becoming apparent several days later. Finally, immunoblots of tissue homogenates from pressure overload-hypertrophied RVs and normally loaded control LVs, using anti-phosphothreonine and anti-phosphoserine antibodies, failed to detect a ~200-kD band (data not shown), such that the MAP 4 of neither hypertrophied nor normal myocardium is significantly phosphorylated on those residues within the basic MAP 4 microtubule binding domain which, when phosphorylated, inhibits MAP 4–microtubule binding (Aizawa et al., 1991). Thus, while a direct cause and effect relationship clearly has not been established, MAP 4 stabilization of the cardiocyte microtubule array would appear to be a logical candidate etiology for the increased microtubule density, and thereby the functional consequence of impaired cardiocyte contractile function, characteristic of pressure overload cardiac hypertrophy.

In counterpoise, however, to this invitingly straightforward linkage of MAP 4 to microtubule stability, are recent data from several non-muscle cultured cell systems. Overexpression of MAP 4 was found to affect neither the quantity nor the assembly of tubulin, nor did it affect microtubule morphology or stability (Barlow et al., 1994). Antibody depletion of MAP 4 was similarly without apparent effect (Wang et al., 1996). While such studies have uncertain relevance to long-term cytoskeletal regulation in the intact organism, they do imply quite clearly that there must at least be redundancy for any microtubule regulatory roles of this structural MAP in the cell types employed. However, the applicability to cardiac and skeletal muscle of this apparently restricted role of MAP 4 in regulating microtubule properties would appear to be quite doubtful, since the striated muscle-specific variant of MAP 4 has an unequivocally obligatory role both in the differentiation and morphogenesis of muscle cells and in the organization of their microtubule array (Mangan and Olmsted, 1996).

In the particular context of the present study it would seem especially unlikely that the upregulation of two functionally related proteins, in the setting of cardiocyte hypertrophic growth wherein changes in the cellular molecular phenotype are minimal, is fortuitous. Thus apart from the direct relationship of MAP 4 to microtubule stability, what linkage might exist? And specifically, why is MAP 4 and tubulin upregulation coordinate, and how does their joint upregulation relate to greater microtubule density? Here, it is of interest that in the course of neuronal development there is coordinate regulation of the expression of the several neuronal MAP isoforms as well as of the multiple α- and β-tubulin isoforms (Oblinger and Kost, 1994). Thus, one can speculate that with hypertrophic cardiac growth re-initiation in specific hemodynamic settings, there may be coordinate upregulation of both MAP and tubulin genes as well as coordinate growth-related changes in isoform expression. In this context, it is notable that while for the most part the α-tubulin and β-tubulin isoforms are functionally equivalent in terms of coassembly into microtubules (Lewis et al., 1987), it is the carboxy-terminal isoform-variable domain of these tubulins that appears to be most important to MAP binding kinetics and, thereby, to microtubule stability (Cleveland, 1987; Maccioni et al., 1988). As an example, again in neuronal systems, a change in the proportion of the three major β-tubulin isoforms has a substantial effect on microtubule stability in these cells (Ludueña, 1993; Panda et al., 1994), such that variation in the ratio of expressed β-tubulin isoforms may represent a means by which the stability of the cellular microtubule array is regulated in response to differing physiological input.

The purpose of this study was to determine whether, in addition to greater tubulin and thus microtubule synthesis, enhanced microtubule stability has a role in the microtubule densification characteristic of the pressure overload-hypertrophied cardiocyte. The two major findings of this study are that the microtubules of these cells exhibit greatly enhanced stability and that this is associated with the upregulation of MAP 4, the major structural MAP of the heart. While it is possible that the earlier and greater upregulation of MAP 4 as opposed to tubulin is driving the increase in microtubule quantity and stability, a direct role for MAP 4 in these functions has not been established here and is in some question, albeit in the restricted context of acute experiments in isolated non-muscle cells. In view both of the interrelated developmental regulation of tubulin and MAP 4 genes, and of the potential for differing β-tubulin isoforms to alter microtubule stability either directly via differing intrinsic properties or indirectly via differing MAP 4 affinities, it will be of considerable interest to determine whether there are isoform-specific changes in cytoskeletal protein gene expression in the pressure-hypertrophied cardiocyte.

We thank E. Nishida and H. Murofushi for antibodies, L. Paturle-Lafanechère for α-tubulin isoform peptides, J. Olmsted for murine MAP 4 cDNA, and Sebette Hamill, Charlene Kerr, and Mary Barnes for their technical assistance. This study was supported by Program Project Grant

HL-48788 from the National Heart, Lung, and Blood Institute and by research funds from the Department of Veterans Affairs.

Received for publication 24 April 1997 and in revised form 10 October 1997.

References

Aizawa, H., Y. Emori, H. Murofushi, H. Kawasaki, H. Sakai, and K. Suzuki. 1990. Molecular cloning of a ubiquitously distributed microtubule-associated protein with Mr 190,000. *J. Biol. Chem.* 265:13849–13855.

Aizawa, H., Y. Emori, A. Mori, H. Murofushi, H. Sakai, and K. Suzuki. 1991. Functional analysis of the domain structure of microtubule-associated protein-4 (MAP-U). *J. Biol. Chem.* 266:9841–9846.

Alonso, A. del C., Arce, C.A., Barra, H.S. 1993. Tyrosinatable and non-tyrosinatable tubulin subpopulations in rat muscle in comparison with those in brain. *Biochim. Biophys. Acta.* 1163:26–30.

Archer, J., and F. Solomon. 1994. Deconstructing the microtubule-organizing center. *Cell.* 76:589–591.

Baas, P.W., and H.C. Joshi. 1992. γ-tubulin distribution in the neuron: Implications for the origins of neuritic microtubules. *J. Cell Biol.* 119:171–178.

Barlow, S., M.L. Gonzalez-Garay, R.R. West, J.B. Olmsted, and F. Cabral. 1994. Stable expression of heterologous microtubule-associated proteins (MAPs) in Chinese hamster ovary cells: evidence for differing roles of MAPs in microtubule organization. *J. Cell Biol.* 126:1017–1029.

Barra, H.S., J.A. Rodriguez, C.A. Arce, and R. Caputto. 1973. A soluble preparation from rat brain that incorporates into its own proteins [^{14}C]arginine by a ribonuclease-sensitive system and [^{14}C]tyrosine by a ribonuclease-insensitive system. *J. Neurochem.* 20:97–108.

Borisy, G.G., J.M. Marcum, J.B. Olmsted, D.B. Murphy, and K.A. Johnson. 1975. Purification of tubulin and associated high molecular weight proteins from porcine brain and characterization of microtubule assembly in vitro. *Ann. NY Acad. Sci.* 253:107–132.

Bulinski, J.C., and G.G. Borisy. 1979. Self-assembly of microtubules in extracts of cultured HeLa cells and identification of HeLa microtubule-associated proteins. *Proc. Natl. Acad. Sci. USA*. 76:293–297.

Bulinski, J.C., and G.G. Borisy. 1980. Microtubule-associated proteins from cultured HeLa cells: Analysis of molecular properties and effects on microtubule polymerization. *J. Biol. Chem.* 255:11570–11576.

Bulinski, J.C., and G.G. Gundersen. 1991. Stabilization of post-translational modification of microtubules during cellular morphogenesis. *Bioessays*. 13: 285–293.

Cleveland, D.W. 1987. The multitubulin hypothesis revisited: what have we learned? *J. Cell Biol*. 104:381–383.

Cooper, G., F.J. Puga, K.J. Zujko, C.E. Harrison, and H.N. Coleman. 1973*a*. Normal myocardial function and energetics in volume overload hypertrophy in the cat. *Circ. Res*. 32:140–148.

Cooper, G., R.M. Satava, C.E. Harrison, and H.N. Coleman. 1973*b*. Mechanism for the abnormal energetics of pressure-induced hypertrophy of cat myocardium. *Circ. Res*. 33:213–223.

Cooper, G., W.E. Mercer, J.K Hoober, P.R. Gordon, R.L. Kent, I.K. Lauva, and T.A. Marino. 1986. Load regulation of the properties of adult feline cardiocytes: The role of substrate adhesion. *Circ. Res*. 58:692–705.

Gundersen, G.G., M.H. Kalnoski, and J.C. Bulinski. 1984. Distinct populations of microtubules: Tyrosinated and non-tyrosinated α-tubulin are distributed differently in vivo. *Cell.* 38:779–789.

Gundersen, G.G., S. Khawaja, and J.C. Bulinski. 1989. Generation of a stable, posttranslationally modified microtubule array is an early event in myogenic differentiaiton. *J. Cell Biol*. 109:2275–2288.

Hill, T.L., and M.W. Kirschner. 1982. Bioenergetics and kinetics of microtubule and actin filament assembly-disassembly. *Int. Rev. Cytol*. 78:1–125.

Joshi, H.C., D. Chu, R.E. Buxbaum, and S.R. Heidemann. 1985. Tension and compression in the cytoskeleton of PC 12 neurites. *J. Cell Biol*. 101:697–705.

Joshi, H.C., M.J. Palacios, L. McNamara, and D.W. Cleveland. 1992. γ-tubulin is a centrosomal protein required for cell cycle-dependent microtubule nucleation. *Nature*. 356:80–83.

Kent, R.L., D.L. Mann, Y. Urabe, R. Hisano, K.W. Hewett, M. Loughnane, and G. Cooper. 1989. Contractile function of isolated feline cardiocytes in response to viscous loading. *Am. J. Physiol.* 257:H1717–H1727.

Kotani, S., H. Murofushi, S. Maekawa, H. Aizawa, and H. Sakai. 1988. Isolation of rat liver microtubule-associated proteins: evidence for a family of microtubule-associated proteins with molecular mass of around 200,000 which distribute widely among mammalian cells. *J. Biol. Chem.* 263:5385–5389.

Kronebusch, P.J., and S.J. Singer. 1987. The microtubule-organizing complex and the Golgi apparatus are co-localized around the entire nuclear envelope of interphase cardiac myocytes. *J. Cell Sci.* 88:25–34.

Lewis, S.A., W. Gu, and N.J. Cowan. 1987. Free intermingling of mammalian β-tubulin isotypes among functionally distinct microtubules. *Cell.* 49:539–548.

Ludueña, R.F. 1993. Are tubulin isotypes functionally significant? *Mol. Biol. Cell.* 4:445–457.

Maccioni, R.B., C.I. Rivas, and J.C. Vera. 1988. Differential interaction of synthetic peptides from the carboxy-terminal regulatory domain of tubulin with microtubule-associated proteins. *EMBO (Eur. Mol. Biol. Organ.) J.* 7:1957–1963.

Mangan, M.E., and J.B. Olmsted. 1996. A muscle-specific variant of microtubule-associated protein 4 (MAP 4) is required in myogenesis. *Development*. 122:771–781.

Mann, D.L., R.L. Kent, and G. Cooper. 1989. Load regulation of the properties of adult feline cardiocytes: Growth induction by cellular deformation. *Circ. Res*. 64:1079–1090.

Mann, D.L., Y. Urabe, R.L. Kent, S. Vinciguerra, and G. Cooper. 1991. Cellular versus myocardial basis for the contractile dysfunction of hypertrophied myocardium. *Circ. Res*. 68:402–415.

McDermott, P.J., L.L. Carl, K.J. Conner, and S.N. Allo. 1991. Transcriptional regulation of ribosomal RNA synthesis during growth of cardiac myocytes in culture. *J. Biol. Chem.* 266:4409–4416.

McNally, F.J., and R.D. Vale. 1993. Identification of katanin, an ATPase that severs and disassembles stable microtubules. *Cell.* 75:419–429.

Oblinger, M.M., and S.A. Kost. 1994. Coordinate regulation of tubulin and microtubule-associated protein genes during development of hamster brain. *Dev. Brain Res.* 77:45–54.

Olmsted, J.B. 1986. Microtubule-associated proteins. *Annu. Rev. Cell Biol.* 2: 421–457.

Ostlund, R.E., J.T. Leung, and S.V. Hajek. 1979. Biochemical determination of tubulin-microtubule equilibrium in cultured cells. *Anal. Biochem*. 96:155–164.

Panda, D., H.P. Miller, A. Banerjee, R.F. Ludueña, and L. Wilson. 1994. Microtubule dynamics *in vitro* are regulated by the tubulin isotype composition. *Proc. Natl. Acad. Sci. USA*. 91:11358–11362.

Paturle, L., J. Wehland, R.L. Margolis, and D. Job. 1989. Complete separation of tyrosinated, detyrosinated, and nontyrosinatable brain tubulin subpopulations using affinity chromatography. *Biochemistry*. 28:2698–2704.

Paturle-Lafanechère, L., B. Edde, P. Denoulet, A. Van Dorsselaer, H. Mazarguil, J.P. Le Caer, J. Wehland, and D. Job. 1991. Characterization of a major brain tubulin variant which cannot be tyrosinated. *Biochemistry*. 30:10523–10528.

Paturle-Lafanechère, L., M. Manier, N. Trigault, F. Pirollet, H. Mazarguil, and D. Job. 1994. Accumulation of Δ2-tubulin, a major tubulin variant that cannot be tyrosinated, in neuronal tissues and in stable microtubule assemblies. *J. Cell Sci.* 107:1529–1543.

Raybin, D., and M. Flavin. 1975. An enzyme tyrosylating α-tubulin and its role in microtubule assembly. *Biochem. Biophphys. Res. Commun*. 65:1088–1095.

Rozich, J.D., M.A. Barnes, P.G. Schmid, M.R. Zile, P.J. McDermott, and G. Cooper. 1995. Load effects on gene expression during cardiac hypertrophy. *J. Mol. Cell. Cardiol*. 27:485–499.

Sanders, M.A., and J.L. Salisbury. 1994. Centrin plays an essential role in microtubule severing during flagellar excision in *Chlamydomonas reinhardtii. J. Cell Biol.* 124:795–805.

Schliwa, M., J. van Blerkom, and K.R. Porter. 1981. Stabilization of the cytoplasmic ground substance in detergent-opened cells and a structural and biochemical analysis of its composition. *Proc. Natl. Acad. Sci. USA*. 78:4329–4333.

Schulze, E., and M.W. Kirschner. 1987. Dynamic and stable populations of microtubules in cells. *J. Cell Biol.* 104:277–288.

Shiina, N., Y. Gotoh, N. Kubomura, A. Iwamatsu, and E. Nishida. 1994. Microtubule severing by elongation factor 1α. *Science.* 266:282–285.

Shiina, N., Y. Gotoh, and E. Nishida. 1995. Microtubule-severing activity in M phase. *Trends Cell Biol*. 5:283–286.

Tagawa, H., J.D. Rozich, H. Tsutsui, T. Narishige, D. Kuppuswamy, H. Sato, P.J. McDermott, M. Koide, and G. Cooper. 1996. Basis for increased microtubules in pressure-hypertrophied cardiocytes. *Circulation*. 93:1230–1243.

Tagawa, H., N. Wang, T. Narishige, D.E. Ingber, M.R. Zile, and G. Cooper. 1997. Cytoskeletal mechanics in pressure-overload cardiac hypertrophy. *Circ. Res.* 80:281–289.

Thompson, W.C., G.G. Deanin, and M.W. Gordon. 1979. Intact microtubules are required for rapid turnover of carboxyl-terminal tyrosine of α-tubulin in cell cultures. *Proc. Natl. Acad. Sci. USA*. 76:1318–1322.

Tsutsui, H., K. Ishihara, and G. Cooper. 1993. Cytoskeletal role in the contractile dysfunction of hypertrophied myocardium. *Science.* 260:682–687.

Tsutsui, H., H. Tagawa, R.L. Kent, P.L. McCollam, K. Ishihara, M. Nagatsu, and G. Cooper. 1994. Role of microtubules in contractile dysfunction of hypertrophied cardiocytes. *Circulation*. 90:533–555.

Wang, X.M., J.G. Peloquin, Y. Zhai, J.C. Bulinski, and G.G. Borisy. 1996. Removal of MAP 4 from microtubules in vivo produces no observable phenotype at the cellular level. *J. Cell Biol*. 132:345–357.

Webster, D.R., J. Wehland, K. Weber, and G.G. Borisy. 1990. Detyrosination of α-tubulin does not stabilize microtubules in vivo. *J. Cell Biol*. 111:113–122.

Wehland, J., and K. Weber. 1987*a*. Tubulin-tyrosine ligase has a binding site on β-tubulin: a two-domain structure of the enzyme. *J. Cell Biol*. 104:1059–1067.

Wehland, J., and K. Weber. 1987*b*. Turnover of the carboxy-terminal tyrosine of α-tubulin and means of reaching elevated levels of detyrosination in living cells. *J. Cell Sci*. 88:185–203.

West, R.R., K.M. Tenbarge, and J.B. Olmsted. 1991. A model for microtubule-associated protein 4 structure: domains defined by comparisons of human, mouse, and bovine sequences. *J. Biol. Chem.* 266:21886–21896.